Isolation, growth, and nitrogen fixation rates of the *Hemiaulus-Richelia* (diatom-cyanobacterium) symbiosis in culture

Amy E. Pyle [1], **Allison M. Johnson** [2], **Tracy A. Villareal** [Corresp. 1]

[1] Department of Marine Science and Marine Science Institute, The University of Texas at Austin, Port Aransas, Texas, United States of America

[2] St. Olaf College, Northfield, Minnesota, United States of America

Corresponding Author: Tracy A. Villareal
Email address: tracyv@austin.utexas.edu

Nitrogen fixers (diazotrophs) are often an important nitrogen source to phytoplankton nutrient budgets in N-limited marine environments. Diazotrophic symbioses between cyanobacteria and diatoms can dominate nitrogen-fixation regionally, particularly in major river plumes and in open ocean mesoscale blooms. This study reports the successful isolation and growth in monocultures of multiple strains of a diatom-cyanobacteria symbiosis from the Gulf of Mexico using a modified artificial seawater medium. We document the influence of light and nutrients on nitrogen fixation and growth rates of the host diatom *Hemiaulus hauckii* Grunow together with its diazotrophic endosymbiont *Richelia intracellularis* Schmidt, as well as less complete results on the *Hemiaulus membranaceus-R.intracellularis* symbiosis. The symbioses rates reported here are for the joint diatom-cyanobacteria unit. Symbiont diazotrophy was sufficient to support both the host diatom and cyanobacteria symbionts, and the entire symbiosis replicated and grew without added nitrogen. Maximum growth rates of multiple strains of *H. hauckii* symbioses in N-free medium with N_2 as the sole N source were 0.74-0.93 div d^{-1}. Growth rates followed light saturation kinetics in *H. hauckii* symbioses with a growth compensation light intensity (E_C) of 7-16 µmol $m^{-2}sec^{-1}$and saturation light level (E_K) of 84-110 µmol $m^{-2}sec^{-1}$. Nitrogen fixation rates by the symbiont while within the host followed a diel pattern where rates increased from near-zero in the scotophase to a maximum 4-6 hours into the photophase. At the onset of the scotophase, nitrogen-fixation rates declined over several hours to near-zero values. Nitrogen fixation also exhibited light saturation kinetics. Maximum N_2fixation rates (84 fmol N_2heterocyst$^{-1}h^{-1}$) in low light adapted cultures (50 µmol $m^{-2}s^{-}$1) were approximately 40-50% of rates (144-154 fmol N_2heterocyst$^{-1}h^{-1}$) in high light (150 and 200 µmol $m^{-2}s^{-1}$) adapted cultures. Maximum laboratory N_2fixation rates were ~6

to 8-fold higher than literature-derived field rates of the *H. hauckii* symbiosis. In contrast to published results on the *Rhizosolenia-Richelia* symbiosis, the *H. hauckii* symbiosis did not use nitrate when added, although ammonium was consumed by the *H. hauckii* symbiosis. Symbiont-free host cell cultures could not be established; however, a symbiont-free *H. hauckii* strain was isolated directly from the field and grown on a nitrate-based medium that would not support DDA growth. Our observations together with literature reports raise the possibility that the asymbiotic *H. hauckii* are lines distinct from an obligately symbiotic *H. hauckii* line. While brief descriptions of successful culture isolation have been published, this report provides the first detailed description of the approaches, handling, and methodologies used for successful culture of this marine symbiosis. These techniques should permit a more widespread laboratory availability of these important marine symbioses.

Isolation, Growth, and Nitrogen Fixation Rates of the *Hemiaulus-Richelia* (Diatom-Cyanobacterium) Symbiosis in Culture

Amy E. Pyle[1,3], Allison M. Johnson, Tracy A. Villareal[1]

[1]Department of Marine Science and Marine Science Institute, The University of Texas at Austin, Port Aransas, Texas, United States of America

[2] St. Olaf College, Northfield, Minnesota, United States of America

Corresponding Author:
Tracy A. Villareal[1],
Marine Science Institute, 750 Channel View Dr, Port Aransas, Texas, United States of America 78373
Email address: tracyv@austin.utexas.edu

16 Abstract

17 Nitrogen fixers (diazotrophs) are often an important nitrogen source to phytoplankton
18 nutrient budgets in N-limited marine environments. Diazotrophic symbioses between
19 cyanobacteria and diatoms can dominate nitrogen fixation regionally, particularly in major river
20 plumes and in open ocean mesoscale blooms. This study reports the successful isolation and
21 growth in monocultures of multiple strains of a diatom-cyanobacteria symbiosis from the Gulf of
22 Mexico using a modified artificial seawater medium. We document the influence of light and
23 nutrients on nitrogen fixation and growth rates of the host diatom *Hemiaulus hauckii* Grunow
24 together with its diazotrophic endosymbiont *Richelia intracellularis* Schmidt, as well as less
25 complete results on the *Hemiaulus membranaceus* -*R. intracellularis* symbiosis. The symbioses
26 rates reported here are for the joint diatom-cyanobacteria unit. Symbiont diazotrophy was
27 sufficient to support both the host diatom and symbiotic cyanobacteria, and the entire symbiosis
28 replicated and grew without added nitrogen. Maximum growth rates of multiple strains of *H.*
29 *hauckii* symbioses in N-free medium with N_2 as the sole N source were 0.74-0.93 div d^{-1}.
30 Growth rates followed light saturation kinetics in *H. hauckii* symbioses with a growth
31 compensation light intensity (E_C) of 7-16 µmol $m^{-2}sec^{-1}$ and saturation light level (E_K) of 84-110
32 µmol $m^{-2}sec^{-1}$. Nitrogen fixation rates by the symbiont while within the host followed a diel
33 pattern where rates increased from near-zero in the scotophase to a maximum 4-6 hours into the
34 photophase. At the onset of the scotophase, nitrogen fixation rates declined over several hours to
35 near-zero values. Nitrogen fixation also exhibited light saturation kinetics. Maximum N_2 fixation
36 rates (84 fmol N_2 heterocyst^{-1} h^{-1}) in low light adapted cultures (50 µmol m^{-2} s-1) were
37 approximately 40-50% of rates (144-154 fmol N_2 heterocyst^{-1} h^{-1}) in higher light (150 and 200
38 µmol m^{-2} s^{-1}) adapted cultures. Maximum laboratory N_2 fixation rates were ~6 to 8-fold higher

than literature-derived field rates of the *H. hauckii* symbiosis. In contrast to published results on the *Rhizosolenia-Richelia* symbiosis, the *H. hauckii* symbiosis did not use nitrate when added, although ammonium was consumed by the *H. hauckii* symbiosis. Symbiont-free host cell cultures could not be established; however, a symbiont-free *H. hauckii* strain was isolated directly from the field and grown on a nitrate-based medium that would not support DDA growth. Our observations together with literature reports raise the possibility that the asymbiotic *H. hauckii* are lines distinct from an obligately symbiotic *H. hauckii* line. While brief descriptions of successful culture isolation have been published, this report provides the first detailed description of the approaches, handling, and methodologies used for successful culture of this marine symbiosis. These techniques should permit a more widespread laboratory availability of these important marine symbioses.

52

53 Introduction

54 The phytoplankton flora of the open sea is a diverse assemblage of prokaryotic and
55 eukaryotic cells that span a size range of ~1 to 2,000+ µm in diameter. Nitrogen is often a
56 limiting nutrient in the open sea, and planktonic nitrogen fixation (diazotrophy) occurs in
57 tropical, subtropical systems and high latitude systems (Zehr 2011; Harding et al. 2018).
58 However, nitrogen fixation can occur in a wide variety of deep-sea and benthic habitats not
59 traditionally associated with nitrogen-limitation (Zehr and Capone 2020). Diazotrophy occurs
60 only in prokaryotic cells, but a variety of symbiotic associations between diazotrophic
61 prokaryotes and host eukaryotes are known (Foster et al. 2006; Foster & O'Mullan 2008; Taylor
62 1982; Villareal 1992; Zehr and Capone 2020) and cover the range from obligate symbioses to
63 loosely associated consorts (Caputo et al. 2019; Carpenter 2002; Foster et al. 2006; Foster &
64 O'Mullan 2008). Of these, diatom-diazotroph associations (DDAs) are the most visible with
65 records dating back to the early 20th century (Karsten 1905).

66 Two types of marine diatom-cyanobacteria symbioses are known: diatoms in the genera
67 *Neostreptotheca* and *Climacodium* that host coccoid cyanobacteria (Carpenter & Janson 2000;
68 Hallegraeff & Jeffrey 1984), and diatoms that host filamentous, heterocyst-forming
69 cyanobacteria of the genera *Richelia* and *Calothrix*. Little is known about the characteristics of
70 the coccoid symbionts in diatoms, although the *Climacodium* symbiont is a diazotrophic
71 *Crocosphaera* sp. (Foster et al. 2011). DDA symbioses involving heterocystous, diazotrophic
72 cyanobacteria are abundant in both open ocean systems (Dore et al. 2008; Villareal et al. 2011;
73 Wilson et al. 2008) and at intermediate salinities within the Amazon (Foster et al. 2007), Mekong
74 (Grosse et al. 2009) and Congo River plumes (Foster et al. 2009). These marine regions differ
75 greatly in their characteristics, suggesting either a great plasticity in physiological responses to

environmental variables or undocumented differentiation within these symbioses. Symbiont integration with the hosts varies as well. In the *Rhizosolenia-Richelia* DDA symbiosis, the symbiont is located in the periplasmic space between the frustule and plasmalemma and has limited contact with the external environment (Janson et al. 1999; Villareal 1989). The *Hemiaulus-Richelia* DDA symbiont is appressed to the nucleus and truly intracellular (Caputo et al. 2019), consistent with its reduced genome (Hilton et al. 2013). The *Chaetoceros-Calothrix* DDA symbiont is completely extracellular to the host diatom (Foster et al. 2010).

Despite their ubiquitous occurrence in tropical seas, the *Hemiaulus-Richelia* symbiosis was largely overlooked until epifluorescence microscopy revealed the cryptic *Richelia* symbiont (Heinbokel, 1986) and N_2 fixation was documented in individually picked chains of the symbiosis (Villareal 1991). In addition to providing fixed N to the pelagic community, diatom-cyanobacteria symbioses play an important role in the nitrogen and carbon cycles of oceanic systems by virtue of their potential to sequester carbon to the deep sea via aggregation and sinking (Karl et al. 2012; Subramaniam et al. 2008). In the currency of oceanic nitrogen cycling, nitrogen derived from photosynthetic nitrogen fixation is generally balanced by a concurrent removal of atmospheric CO_2 (Eppley & Peterson 1979). Thus, sinking material fueled by phototrophic diazotrophy represents a net removal of CO_2, and is a quantitatively important process in the transport of carbon to depth. DDAs, and particularly *Hemiaulus* symbioses, are of particular oceanographic significance. *Hemiaulus-Richelia* symbioses bloom at ~ 10^3 cells L^{-1} frequently at the Hawai'i Ocean Time-series HOT (Dore et al. 2008; Fong et al. 2008; Scharek et al. 1999; White et al. 2007). At this location, they are the likely source of the summer export pulse that provides 20% of the annual carbon flux to 4,000 m in a 4-6-week window (Karl et al. 2012) and are regularly found on sinking particles (Farnelid et al. 2019). Subtropical front

blooms at ~28-30°N in the Pacific (Venrick 1974; Villareal et al. 2012; Wilson et al. 2004; Wilson et al. 2008) and in waters west and north of HI (Brzezinski et al. 1998; Villareal et al. 2011) suggest a basin scale significance. In the southwest Atlantic Ocean, *Hemiaulus hauckii-Richelia* blooms cover 10^5+ km^2 and sequester 1.7 Tmol of carbon annually (Carpenter et al. 1999; Subramaniam et al. 2008) and CO_2 drawdown effects can extend to 10^6 km^2 (Cooley et al. 2007). The large size, chain-formation, and tendency to aggregate (Scharek et al. 1999; Villareal et al. 2011) in the host *Hemiaulus* lead to an efficient export mechanism (Yeung et al. 2012) for both N and C.

Culture studies on the growth and physiological characteristics of these symbioses are limited. The external symbiont *Calothrix rhizosoleniae* has been cultured without its host (Foster et al. 2010) in both natural and artificial seawater medium. Cultures of the *Rhizosolenia-Richelia* symbiosis using amended seawater have been reported in the literature with growth rates up to 0.8 div d^{-1} in fixed N-free medium (Villareal 1990). In the *Rhizosolenia-Richelia* DDA, host and symbiont growth can be independent and symbiont-free host cells occur (but have reduced growth rates) even when no fixed N is present, possibly through use of N excreted by *Richelia* into the medium. Addition of nitrate rapidly results in the loss of symbionts as asymbiotic *Rhizosolenia* uses the added nitrate, increases its growth rate, and out-competes symbiotic *Rhizosolenia-Richelia* (Villareal 1989; Villareal 1990). Nitrogen fixation follows typical light saturation kinetics and can provide the entire N needs of the symbiosis (Villareal 1990). Although oceanographically more significant than other *Rhizosolenia-Richelia* DDA (Heinbokel 1986; Subramaniam et al. 2008, Villareal 1992), there are no published culture-based data for the *Hemiaulus-Richelia* symbiosis.

Using nano-SIMS on field samples, Foster et al. (2011) were able to document the transport of recently fixed N from the symbiont *Richelia* to the host *Hemiaulus* in sufficient quantities to support growth; however, it is not known whether *Hemiaulus*-*Richelia* can grow exclusively on diazotrophically fixed N. Regardless, the symbiont is clearly advantageous to the host since, where examined, 80-100% of the *Hemiaulus* contain the symbiont (Bar-Zeev et al. 2008; Heinbokel, 1986; Villareal 1991; Villareal 1994) and 85-100% of the total phytoplankton N needs in the Amazon River plume can be met by *Hemiaulus* DDA diazotrophy (Carpenter et al. 1999; Weber et al. 2017). The symbiosis is not obligate for the host *Rhizosolenia* in DDA cultures (Villareal, 1990) and the field evidence suggests this may also be true for the host *Hemiaulus* (Heinbokel, 1986; Kimor et al., 1978). This latter hypothesis has not been tested due to the difficulty in growing the *Hemiaulus*-*Richelia* host-symbiont pair *in vitro*.

In this paper, we report the successful isolation of two species of the *Hemiaulus*-*Richelia* symbiosis into culture and expand on the brief culturing description reported in Schouten et al. (2013). Using primarily *H. hauckii*-*Richelia* DDA strains, we document light-dependent growth rates, diel cycles of N_2 fixation, growth rate response to various forms of added nitrogen, and N_2 fixation rates. These parameters are essential to supporting modeling of DDA bloom formation and fate (Follett et al. 2018; Stukel et al. 2014). In addition, key differences between the *Hemiaulus* and *Rhizosolenia* DDAs are noted.

Methods and Materials

All culturing was conducted at the University of Texas Marine Science Institute (UTMSI) in Port Aransas, Texas. *Hemiaulus* strains containing symbionts were isolated by micropipette (Andersen & Kawachi 2005) from the Port Aransas ship channel (27° 57’ 17.56” N, 90° 03” 00.48” W) using material from either net tows (20-35 μm mesh nets, 1-3 minute tows in the

144 incoming tide) or whole water samples (incoming tide). The net tow sample was collected from a
145 platform under a pier laboratory that both shaded the sample from direct sun the entire time as
146 well as facilitating numerous short tows resulting in dilute samples. Both initial isolations and
147 subsequent cultures of symbiont containing *Hemiaulus* were maintained in sterile filtered, fixed
148 N-free YBCII media with L1 trace metal/ EDTA additions (Ohki et al. 1992; Chen et al. 1996;
149 Guillard & Hargraves 1993), and final concentrations of 1 µM sodium glycerophosphate
150 ($C_3H_7Na_2O_6P$), 2.6 µM sodium dihydrogen phosphate monohydrate ($NaH_2PO_4 \cdot H_2O$) and 35.7
151 µM sodium metasilicate ($Na_2SiO_3 \cdot 9H_2O$). Throughout the text, N-free or fixed N-free medium
152 will refer to culture medium that has no added organic or inorganic N, recognizing that dissolved
153 N_2 will be abundant as an N source for diazotrophs. Sterile filtered medium and seawater were
154 generated using commercially available sterile tissue culture towers and reservoirs (0.22 µm pore
155 size filters). Sterile filtration units were rinsed with ~50 ml of medium prior to use for culture
156 medium. Both nylon and methyl cellulose 0.22 µm pore size filters were used with no apparent
157 difference in results. All chemicals were reagent grade or better. The modified YBCII medium
158 was checked with a hand-held refractometer before each use and adjusted to a salinity of 35 as
159 needed using 18 megaohm deionized water. Autoclaved tubes were rinsed with sterile filtered
160 medium and then the tube filled with 15-20 mL of medium. This rinsing step was used for all
161 flasks and tubes used for culturing.

162 Isolations were performed within 5-10 minutes of collection. Using a stereomicroscope,
163 multiple *Hemiaulus* chains were rapidly isolated from the net tow material using hand-held
164 borosilicate pipets drawn to a fine diameter in a gas flame. In our work, the drawn-out pipets
165 were attached to tubing to a cotton-plugged mouthpiece (to prevent seawater aspiration) of fire-
166 polished glass tubing. Mouth pipetting was used to carefully draw or expel the chain. If mouth

pipetting is unacceptable, any form of fine control would provide adequate results. Multiple *Hemiaulus* chains were isolated into one well of a glass depression well plate (16 depressions) containing ~2 ml of medium per depression. Individual chains were then rinsed via serial transfer into other wells containing sterile medium. Extensive rinsing (5-6 rinses) of a single chain before isolating the next chain was much less successful than only 2-3 rinses before placing the chain into a tube of medium. When isolated directly into the N-deplete modified YBCII medium, contaminant growth was minimal even with only 1-2 rinses. These techniques resulted in symbiosis isolation free of other eukaryotes or cyanobacteria in ~30-40% of the attempts. Preliminary experiments used *H. hauckii* strain #9 isolated during Spring 2010. Subsequent *H. hauckii* experiments used isolates established during Fall 2010 (strain #22) and Fall 2011 (strain #83, #91, and #92). *Hemiaulus membranaceus* strain #82 was isolated in the Fall 2011. In all subsequent text, a strain designation indicates a culture of a host diatom containing one or more symbionts. While *Hemiaulus hauckii* strain #91 was used for most of the experiments, a single strain for the entire suite of experiments was not possible due to loss of the strain or the periodic loss of vitality noted in the results. Strains used are identified in the text and in Table S1.

The *Hemiaulus* DDA could be isolated for short-term growth into MET-44 (Schöne and Schöne 1982) nutrient-amended sterile filtered seawater (0.22 μm filter equipped commercial sterile filtration units) collected at the isolation point. However, the *Hemiaulus-Richelia* symbioses required re-isolation from the MET-44 medium into the modified YBCII medium for successful maintenance >2-3 weeks. After isolation, cells were placed in a 25 °C incubator under cool white fluorescent illumination of 150-250 μmol m^{-2} sec^{-1} on a 12:12 Light:Dark (L:D) cycle. All cultures were grown as batch cultures. Cultures had a high rate of sudden

decline and death when kept in medium longer than 7-10 days and careful attention was required to transfer the cultures to new medium within this time frame. Experiments were initiated within 6 months of culture isolation; cultures failed to make auxospores and were eventually lost after approximately 1-2 years in culture. No attempt was made to culture axenically; bacteria were rarely visible in the cultures under phase contrast or differential interference contrast optics until senescence when cell mortality was substantial. *The H. hauckii* DDA was the primary experimental tool. *Hemiaulus membranaceus* DDA cultures were examined for general characteristics but were not the subject of intensive experimentation. In March 2017, *Hemiaulus* chains were observed in the Port Aransas ship channel from the Imaging Flow Cytobot data stream (Campbell et al. 2010, 2017). Examination of net tow material noted numerous asymbiotic *H. hauckii* chains and no symbiotic cells. Asymbiotic chains of *Hemiaulus hauckii* were isolated into N-replete (40 µm NO_3^-) MET-44 amended sterile filtered seawater as noted above. Unless otherwise noted, all experiments were conducted using modifies YBCII medium with no added nitrogen. Dissolved N_2 was the only available nitrogen source.

Analytical methods

Cells were counted using a S52 Sedgewick-Rafter chamber on an Olympus BX51 epifluorescence microscope. Excitation/emission wavelengths for the epifluorescent filters used in counts and photography were 450 nm/680 nm (chlorophyll *a*), and 490 nm/ 565 nm (phycoerythrin). Both host cells and symbiont trichomes/heterocysts were enumerated. Percent symbiosis was calculated as the number of diatoms containing one or more *Richelia* trichomes divided by the total number of potential host cells. Growth rates (reported as div d^{-1}) were calculated using daily counts as the slope of the log of cell number over the change in time

(Guillard 1973) with the 95% confidence interval around the slope of the line calculated in Microsoft Excel.

Acetylene reduction assays (ARA) were performed as described in Capone (1993) corrected for ethylene solubility as described by Breitbarth et al. (2004) and assuming a mol ethylene reduced per mol N_2 conversion ratio of 4:1 (Jensen & Cox 1983 as modified by Capone 1993). An SRI 8610C gas chromatograph (SRI Instruments, Torrance, CA) equipped with a 30 cm silica gel column was used to quantify ethylene using a commercially prepared standard (GASCO Safeware Precision Gas Mixture, 10 and 100 ppm). Manufacturer-provided software (PeakSimple Chromatography Software) performed peak integrations. Standards were run prior to each day's run and at several points during the experiment. For each assay, 15 ml of culture sample was added to an acid-washed 25 ml incubation vial fitted with a grey chlorobutyl rubber serum stopper and crimped aluminum seals leaving 10 ml of headspace. Sterile-filtered medium was used as a control. A separate aliquot was retained for cell counts. One ml of acetylene generated from calcium carbide (Capone 1983) was introduced, gently swirled for 15-30 seconds to equilibrate while minimizing contact between the serum stopper and the culture, then 100 µL of the vial headspace injected with a Hamilton gas-tight syringe and injected into the GC. Each injection required 5-7 minutes after an injection to return to baseline.

Chlorophyll *a* was determined on methanol-extracted (24 hours, -20°C) samples (10-25 ml aliquot) collected on 0.4 µm pore size polycarbonate filters using a non-acidification method (Welschmeyer 1994). Initial tests indicated the filters used did not leach fluorescent compounds in the methanol. When chl *a* cell^{-1} is referred to, it always includes both symbiont and host chl *a*. Sample fluorescence was read on a TD-700 Fluorometer (Turner Designs, CA, USA).

For nutrients, a 25 mm, 0.22 µm pore-size membrane cellulose ester Millipore filter mounted on a syringe was rinsed with 5 ml of sample, filtrate discarded, and ten ml of sample medium was filtered and frozen. A SEAL Analytical QuAAtro autoanalyzer was used to determine dissolved inorganic phosphate (DIP), nitrate +nitrite (N+N), ammonium (NH_4^+), and silicate (SiO_4^{-2}) concentrations using the manufacturer's recommended chemistries. The chemistries are similar to automated analyses published in Grasshoff et al. (1999) with changes in reagent concentration and wetting agents specific to the manifold chemistries. Detection limits were ~0.05 µM for N+N, NH_4^+ and P, and ~0.5 µM for Si.

Growth-rate and N_2 fixation versus irradiance experiments

H. hauckii symbiosis strains #9 and #91 were used for the irradiance-rate experiments. Initial experiments (Strain #9) used two light levels and are included for comparison. Detailed growth rates and N_2 fixation rates were measured in separate experiments using 7-8 different light levels (photosynthetic photon flux density) ranging from 15-600 µmol m^{-2} sec^{-1} measured by a QSP-170B irradiance meter (Biospherical Instruments; Table S1). For growth rates, cultures were grown at the 7 experimental light levels for 7 days and remained at the assigned light level through the duration of the experiments. Symbiosis growth is used throughout this paper to refer to increases in host diatom numbers containing at least one symbiont. For N_2 fixation, strains were adapted to either 50, 150, or 200 (high light HL) µmol m^{-2} sec^{-1} at 25°C and a salinity of 35 under cool white fluorescent lighting for 7 days prior to the acetylene reduction assay. Each adaptation level was then exposed to 7-8 light levels for acetylene reduction assay

Diel pattern of N_2 fixation

256 *H. hauckii* strains #22 and #92, and *H. membranaceus* strain #82 were used for the diel
257 study (12:12 L:D cycles at 200 µmol $m^{-2}sec^{-1}$) examining the daily rhythm of N_2 fixation on
258 culture medium with no added N. Initial experiments on *H. hauckii* strain #22 utilized a set of 6
259 discrete time points between 0600 to 2100. Each incubation lasted 4 hours with initial and final
260 measurements taken in triplicate. Rates were normalized to heterocysts and used the center point
261 of the 4 h incubation period as the time stamp. Subsequent experiments on *H. hauckii* strain #92
262 and *H. membranaceus* strain #82 utilized a high frequency time series approach in order to
263 resolve changes occurring on an hourly basis or less. This approach used a series of individual
264 measurements taken from a single vial over a period of up to ~12 hours and was utilized for two
265 reasons. First, individual assays injections required 5-7 minutes to return to baseline. Triplicate
266 measurements therefore required 15-21 minutes during which ethylene production was occurring
267 at measurable rates, could not be consideration true replication of the ethylene measurement.
268 Averages of these triplicates would be unable to resolve rate changes on short time scales. The
269 second reason for this approach was to minimize handling, agitation, and light/temperature
270 variation of the samples. Six (*H. hauckii*) or 8 (*H. membranaceus*) paired vials were started at
271 various time points in the diel cycle to permit overlap. Individual time series can be identified
272 from the labelling in Table S1. Vials were sampled sequentially (1a, 1b, 2a, 2b, 3a,3b, then
273 repeated) yielding approximately 1-1.5 hours between successive sampling of a single vial. The
274 difference between successive measurements (ethylene per heterocyst) was normalized to the
275 time difference between the two successive points (~1 -1.5 hours) and expressed as a rate
276 (ethylene $heterocyst^{-1}$ $time^{-1}$). Eighty-nine (*H. hauckii)* and 78 (*H. membranaceus)* separate
277 measurements were plotted against time using a 5-point running average (center point plus two
278 on either side) to smooth the data. Rates from different vial series overlapped in time, thus the

5-point average has rates from independent time series. Standard deviation was calculated on this 5-point series recognizing this is not a statistically useful value but only a metric for the noise in the data. Experimental cultures were adapted to at 25° C under 200 μmol m^{-2} s^{-1} illumination (cool-white fluorescence bulbs) on 12:12 LD cycle. Experimental vials were incubated under these same conditions. Samples during the scotophase were collected/returned to the incubator in a darkened container and shielded from the dimmed laboratory lights during the assay.

Nutrient addition experiments

Nitrogen source experiments addressed the effect of various inorganic N sources on symbiosis growth and N_2 fixation. In these experiments, *H. hauckii* strain # 83 was transferred to three 2 L autoclaved glass Erlenmeyer flasks containing the maintenance medium listed above amended with one of the following nitrogen sources: no added nitrogen (control), added nitrate (40μM) or added ammonium (10μM). Samples were maintained at 25 °C and a salinity of 35. Reduced ammonium concentrations were used to avoid toxicity effects; the nitrate concentration duplicated work on the *Rhizosolenia-Richelia* symbiosis (Villareal 1989). Nutrient concentrations and cell abundance were sampled 10 times throughout the duration of the 20-day experiment. Nutrient analyses and cell counts were done in duplicate.

Curve-fitting and Statistics

Light-dependent growth was fit to the Jassby-Platt hyperbolic tangent function (Jassby & Platt 1976) with a y-intercept term to permit calculation of compensation light intensity. The y-intercept term was omitted for the N_2 fixation rates versus irradiance curves due to time-dependent decline in dark N_2 fixation that became evident in the diel measurements. When not omitted, the time-dependent decline in dark N_2 fixation noted in the diel experiment at the

beginning of the scotophase resulted in a highly variable initial slope as well as a significant y-intercept (dark fixation rate) that was not consistent with the longer term rates after several hours in darkness. Delta Graph (Red Rocks Software) was used for graphics as well as curve fitting of the growth and N_2-irradiance curves. T-tests were performed using the data analysis package in Microsoft Excel. Confidence intervals or standard deviations (noted in text) were calculated using Microsoft Excel software. Data from all figures are found in Table S1.

Results

Hemiaulus hauckii and *Hemiaulus membranaceus* with their symbiont *Richelia intracellularis* were successfully isolated multiple times. We found it was essential to remove the *Hemiaulus* from the net tow sample as quickly as possible (3-5 minutes after completion of the tow). Successful culturing resulted in rapidly growing chains of *Hemiaulus* reaching over 80 cells in length (Fig. 1). Multiple symbionts (usually 1-2, but never more than 4) were evident in the cells. Cultures were sensitive to handling, and swirling tubes to re-suspend chains resulted in chain breakage and decreased growth rates. Growth in undisturbed large volume containers (10 L+) resulted in complex aggregate formation. Strains were difficult to ship, and only one attempt out of approximately 15 resulted in successful establishment in another facility. A single auxospore-like structure was observed, but no cell diameter increases were observed in any of the cultures.

H. hauckii strains used in this study ranged from 12-17.5 µm (up to 30 µm observed) in diameter (pervalvar axis presented in broad girdle view) with a total cell volume range of 7,012 – 23,574 μm^3. *H. membranaceus* cells were not measured. Since auxosporulation did not occur, the strains gradually decreased in diameter over a period of 1-2 years and eventually died out. Individual strains exhibited periods (weeks/months) of healthy growth (0.5-0.9 div d^{-1}) with little care required. This growth pattern was interspersed with intervals (days/weeks) of low growth rates that required substantial attention and multiple backups to prevent loss of the culture. These cyclic patterns were not linked to batches of culture medium or glassware. While not enumerated, bacteria were rarely evident in light microscopy but certainly present since the cultures were not axenic. Reasons for the observed growth pattern variability remain unknown.

Individual symbiosis strains were routinely maintained in modified YBC-II medium with no added nitrogen. High densities of *Hemiaulus* and its symbionts were possible with no N added to the synthetic seawater medium (residual combined inorganic N < 0.1 μM). Maximum cell counts of the host *H. hauckii* reached ~10,000 cells mL^{-1} with a maximum chl *a* concentration of 71 μg L^{-1}. Typical cell and chl *a* dynamics are shown in Fig. 2. High light (200 μmol m^{-2} s^{-1}) chl *a* concentration reached a maximum approximately 3.5 times greater than the low light (50 μmol m^{-2} s^{-1}) concentrations, although chl *a* per symbiosis (combined host and symbiont; multiple strains) remained approximately equal over time. In both light conditions, chl *a* per symbiosis was maximal (~4-5 pg chl *a* $symbiosis^{-1}$) in early exponential growth and declined over time to ~2-3 pg chl *a* $symbiosis^{-1}$. Extensive chain formation resulted in a high degree of variation in measurements.

Growth rates of *H. hauckii* in N-deplete medium (Fig. 3) followed light saturation kinetics with host and symbiont growth rates highly correlated (r^2= 0.98, p=0.05, t-test). Photoinhibition was not observed at the maximum light level used (500 μmol m^{-2} s^{-1}). A modified Jassby-Platt curve fit (Article S1) yielded a realized maximum growth rate μ of 0.74-0.93 div d^{-1} in replicated experiments (Fig. 3, Table 1). Light-saturated growth occurred with light saturation (E_k) occurring at 84-110 μmol m^{-2} s^{-1} and an initial slope (α) of 0.009 div d^{-1}(μmol m^{-2} s^{-1})$^{-1}$ in both irradiance curves. Compensation light intensity (E_c) calculated from the y-intercept and α varied from 7-16 μmol m^{-2} s^{-1}.

Nitrogen fixation rates estimated by acetylene reduction were tightly linked to the light:dark cycle (Fig. 4). The 5-point running average was necessary to smooth the variable point-to-point time series rates into a general diel curve. Two separate experimental treatments (the 4-hour incubations and the 5-point averaging series) indicated the maximum acetylene

353 reduction rate in both *H. hauckii* and *H. membranaceus* DDA occurred approximately 4 hours
354 into the photophase (12:12 photoperiod) with a broader maximum acetylene reduction rate
355 extending for 4-6 hours. Acetylene reduction declined over several hours at photophase end to
356 low (1-10% maximum values) but still measurable rates during the scotophase in both *H. hauckii*
357 (Fig. 4a) and *H. membranaceus* (Fig. 4b) DDAs. Unlike the 4-hour discrete incubation diurnal
358 pattern seen in Strain #22, *H. hauckii* strain #92 rates maintained high values until the end of the
359 photophase (Fig. 4a). *Hemiaulus membranaceus* DDA rates were more symmetrically
360 distributed around the middle of the photoperiod (Fig. 4b). In both data sets, the rates reached a
361 maximum in the range of 45-55 fmol N_2 heterocyst^{-1} h^{-1}.
362 Nitrogen fixation-irradiance rates followed a light saturation curve (Fig. 5) fit to the
363 hyperbolic tangent function. At the 150 and 200 µmol m^{-2} s^{-1} adaptation level (r^2=0.95 and 0.97,
364 respectively), the curve-fit maximum N_2-fixation rates was 155 and 144 fmol N_2 heterocyst^{-1} h^{-1},
365 respectively. The maximum rates (light-saturated) at 150 and 200 µmol m^{-2} s^{-1} adaptation level
366 were significantly ($p<0.01$, t-test) greater than the maximum (light-saturated) rate (86 fmol N_2
367 heterocyst^{-1} h$^{-1)}$ noted in cultures adapted to 50 µmol m^{-2} s^{-1}. The initial slope (light limited
368 portion) of the N_2 fixation curve was approximately 75% higher in the 50 µmol m^{-2} s^{-1} adapted
369 culture than the 150 and 200 µmol m^{-2} s^{-1} adaptation level.
370 Preliminary experiments in 2010 found that *H. hauckii* strain #9 did not utilize nitrate
371 (Table S2). Subsequent replication experiments found that 40 µM nitrate was not used by a
372 different *H. hauckii* symbiosis strain (#83) in experiments conducted 1 year later (Fig. 6). Ten
373 µM added ammonium declined to ~0.4 µM in 13 days and then remained constant thereafter
374 (Fig. 6). *Hemiaulus hauckii* strain #83 drew down P and Si under all the available N sources at
375 approximately equal rates. The addition of ammonium in an experimental comparison resulted in

higher percentages (up to 48%) of asymbiotic cells in exponential growth than when either nitrate (10-20%) was added or no N was present in the medium (10-20%) but the strain was not grown free of its symbiont (Fig. 6).

A symbiont-free strain of *H. hauckii* was maintained from March 2017 to August 2017 on a solely nitrate enriched, natural seawater medium (MET-44; Sch. Ammonium concentrations in the aged stock seawater were 0.5 μM or less. When isolated and growing, it was confirmed in April 2017 to be symbiont-free by epifluorescence microscopy and maintained in a seawater-based culture medium (MET-44) that would not support the DDA strains. The strain was lost during Hurricane Harvey in August 2017 and no further information was collected.

Discussion

Physiology and rate measurements of *Hemiaulus* symbioses have previously been limited to field collected and incubated samples. Using a modification of an artificial seawater medium, we have successfully and reproducibly cultured two species of *Hemiaulus* with their symbiont. Caputo et al. (2019) also reported brief success using an artificial medium; Hilton et al. (2013) reported genetic sequences from *Richelia* extracted from *Hemiaulus* grown using these methods.

Greatest isolation success was found when the cells were rapidly removed from the net tow cod-end, suggesting sensitivity to the various exudates found in these concentrated samples. In addition, the seawater was sterile filtered rather than autoclaved or pasteurized. Sterile filtration leaves the carbonate system and medium pH unaltered compared to heat treatment; however, viruses are not inactivated. Little is known of virus/DDA interactions, but viruses play

398 a significant role in diatom mortality in general (Kranzler et al. 2019) and could be a problem for
399 stable cultures.

400 In addition, culture media designed to support phytoplankton may not support essential
401 phycosphere components or may support difficult to remove lethal bacteria (see van Tol et al.
402 2017 for an example). The inability to culture *Hemiaulus* in a seawater-based enrichment
403 medium used for concurrent *Rhizosolenia-Richelia* cultures suggests that the additional trace
404 metal and chelation in our modified YBCII medium was required for sustained growth or that
405 water quality issues are critical. While we did not perform systematic comparisons, seawater
406 from the Port Aransas pass is heavily influenced by both the inshore bays and coastal Gulf of
407 Mexico. Our modified YBCII medium is free of these influences and we speculate provides a
408 more consistent chemical environment. These difference highlights differing growth needs,
409 sensitivities or tolerances of the *Hemiaulus* and *Rhizosolenia* DDAs that remain to be described.
410 The oscillation between rapidly growing, apparently healthy cultures and less vigorous cultures
411 is clearly an impediment to sustained culture as is the lack of auxospore formation. None of the
412 isolations persisted for more than ~ 3 years making detailed work on model strains problematic
413 at this time.

414 Previous estimates of N_2 fixation tracked ^{15}N isotope movement from the *Richelia*
415 symbiont heterocysts to the host *Hemiaulus* cells using single-cell methods (Foster et al. 2011)
416 and estimated that it was sufficient to support cell growth with a turnover time of up to 0.59 div
417 d^{-1}. Foster et al.'s (2011) rate measurements for *H. hauckii-Richelia* (n=17) averaged 20.4 ±
418 18.5 (std. dev.) fmol N heterocyst^{-1} h^{-1} (range 1.15-50.4 fmol heterocyst^{-1} h^{-1}). These
419 heterocyst normalized rates (Foster et al.'s Table 1 footnote), are lower than the rates observed in
420 the cultures (up to 155 fmol N_2 heterocyst^{-1} h^{-1}). Our culture growth rates (non-limiting

421 conditions) suggest some degree of limitation in their field collections. Light/ growth rate
422 adaptation to 150-200 µmol m^{-2} s^{-1} PAR was concurrent with a maximum N_2 fixation rate
423 approximately 6 times higher than the maximum rates observed by Foster et al. (2011).
424 Data digitized (Plot Digitizer from SourceForge, Slashldot Media, 225 W. Broadway,
425 Suite 1600, San Diego, CA: https://sourceforge.net/) from Carpenter et al.'s (1999) Fig. 2, allows
426 comparison of our symbiosis culture N_2 fixation rates to those from an Amazon River plume
427 bloom where *Hemiaulus* DDA abundance reached 1.6 X 10^6 heterocysts L^{-1}. After extracting
428 their N_2 fixation rates (as mg N m^{-2} d^{-1}) and concurrent heterocyst abundance from Carpenter et
429 al.'s (1999) Fig. 2, we determined that their rates ranged from 0.6-40.3 fmol N heterocyst^{-1} h^{-1}
430 and were ~8 fold lower than the maximum rates seen in cultures (note the unit conversion and
431 comparison: mg N, fmol N or fmol N_2 fixed). These rates were generated from material
432 collected by net and then prescreened to remove *Trichodesmium*. Based on our isolation
433 attempts, this handling probably adversely affected the rate. Carpenter et al. (1999) also reported
434 undetectable nitrate uptake in the *Hemiaulus* DDA bloom, a result consistent with our culture
435 observations that these DDA strains did not utilize nitrate.
436 Many growth characteristics of *H. hauckii-R. intracellularis* are similar to the
437 *Rhizosolenia clevei-R. intracellularis* symbiosis. Maximum growth rates are slightly less than 1
438 div d^{-1} and are similar between the two DDAs despite their significant size difference. Growth
439 rates are not photoinhibited up to 500 µmol photons m^{-2} s^{-1}. Rapidly growing cells form
440 extensive chains. Culture agitation, albeit qualitatively measured, negatively affects chain
441 formation and possibly growth rates. The diel pattern of nitrogen fixation in the *Hemiaulus* DDA
442 cultures parallels the diel nifH nitrogenase gene expression seen in field samples of both
443 *Hemiaulus* DDAs (Zehr et al. 2007), the *Rhizosolenia* DDA (Harke et al. 2019) and both gene

444 expression and acetylene reduction in the *Calothrix* symbiont of the *Chaetoceros* DDA (Foster et
445 al. 2010).

446 The differential nitrate use by the *Hemiaulus* and *Rhizosolenia* DDAs is a significant
447 difference between the two DDAs. Preferential NO_3^- utilization drove a higher host growth rate
448 in a strain of the *Rhizosolenia* DDA, eventually leading to symbiont-free host cultures (Villareal
449 1990) growing solely on NO_3^-. In field studies where N_2 appeared to be the primary N source,
450 the *Rhizosolenia* host and symbiont DDA were tightly coupled (Harke et al. 2019). There are at
451 least two mechanisms that could produce this result in the *Rhizosolenia* DDA: downregulation of
452 symbiont diazotrophy by exposure to NO_3^- due to its extra-plasmalemma location and/or
453 induction of host nitrate reductase pathways. The latter would result in diminished carbon flow
454 to the symbiont in order to support nitrate assimilation into protein. Neither of these mechanisms
455 appear to have occurred in the *H. hauckii* DDA strains we used. These results were replicated in
456 individual experiments four years apart on different strains, excluding the possibility that the
457 results were a laboratory condition artifact. For the *Hemiaulus* DDA, either nitrate cannot be
458 used or diazotrophic supply exceeded any immediate N demand by the symbiosis and suppressed
459 NO_3^- uptake. In contrast, ammonium was used and resulted in elevated percentages of symbiont-
460 free hosts, but not a symbiont-free culture. The free-living marine cyanobacterium
461 *Trichodesmium* can use NO_3^- either preferentially or concurrently during diazotrophy as an N
462 source (Holl & Montoya 2005; Klawonn et al. 2020; Mulholland & Capone 2000) and other
463 diazotrophs can simultaneously use N_2 and NO_3^- (Inomura et al. 2018). It is unusual for NO_3^-
464 not to be used at all due to the higher overall energetic cost of nitrogen fixation added to the
465 costs maintaining specialized cellular structures in diazotrophs (Inomura et al. 2018). However,
466 in the UCYN-A/haptophyte symbiosis, the host haptophyte only assimilates diazotrophically

fixed N_2 even in the presence of combined DIN (Mills et al. 2020). Thus, while unusual, the *H. hauckii-Richelia* symbiosis is not unique. The truly intracellular location of the *Hemiaulus* symbiont (Caputo et al. 2019) clearly limits its contact with the environment and the potential impact of NO_3^-, but our observations also require the host *Hemiaulus* to be unresponsive to external nitrate.

In contrast, *Hemiaulus* spp. (no information on symbionts) has been reported with growth rates up to 2.2 div d^{-1} (Furnas 1991) in field experiments and 3.8 div d^{-1} in nitrate-based laboratory medium (Brand & Guillard 1981). While the symbiont presence is undocumented but seems unlikely given the DDA growth rates reported in our paper of <1.0 div d^{-1} as well as by modelled symbiont diazotrophy (Inomura et al. 2020). The Furnas (1991) and Brand & Guillard (1981) reports, as well as our briefly established asymbiotic strain on medium that would not support *Hemiaulus* DDA growth, all suggest that symbiont-free strains of *Hemiaulus* are extant in the modern ocean. *Hemiaulus* DDAs had an ancestral origin 50-100 million years ago (Caputo et al. 2019), but asymbiotic *H. hauckii* strains apparently still persist in the modern ocean. We suggest this data supports, but does not prove, that the *Hemiaulus* DDA, with its close metabolic coupling of the host-symbiont nitrogen metabolism (Foster & Zehr 2019; Hilton et al. 2013), is obligate and that symbiotic host *Hemiaulus* spp. are distinct from asymbiotic *Hemiaulus* strains. These asymbiotic strains should provide an invaluable tool for examining evolutionary processes in DDAs.

The growth rate and N_2 fixation results provide useful input to models examining the biogeochemical impact of the *Hemiaulus* DDA blooms in oceanic regions. The Amazon River plume is particularly noteworthy in that it has an explicit model describing the ecological-biogeochemical impacts. Stukel et al.'s (2014) model incorporated high generic N_2-based DDA

490 growth rates > 1 div d^{-1} with asymbiotic cells growing on ambient N at somewhat greater rates.
491 Our experimental results are much lower for growth on N_2 (maximum ~0.9 div d^{-1}) and indicated
492 no nitrate use. Non-diazotrophic, asymbiotic *Hemiaulus* growth rates from the literature are
493 much higher than N_2-based DDA rates. These are significant alterations in the input values
494 available to Stukel et al. (2014).
495 In addition, our results for *H. hauckii* DDAs found no evidence of growth rate
496 photoinhibition at the highest light level used (500 µmol m^{-2} s^{-1}). While instantaneous solar
497 PAR may reach ~2,000 µmol m^{-2} s^{-1} (Björkman et al. 2015) at Station ALOHA near Hawaii (22°
498 45' N 158° 00' W), average daily PAR incident at Sta. ALOHA over the diurnal is ~850 µmol
499 m^{-2} s^{-1} from June-Aug. (calculated from Letelier et al. 2017). Vertical mixing rates will both
500 reduce the time averaged PAR exposure exponentially with the depth of mixing as well as being
501 rapid enough to preclude general phytoplankton photoacclimation (Tomkins et al. 2020). Thus,
502 it seems possible that *in-situ* PAR values would not photoinhibit these DDA strains. However,
503 damaging effects by solar UV wavelengths (Zhu et al. 2020) require further examination.
504 Follet et al. (2018) and Inomura et al. (2020) utilized *H. hauckii* DDA growth rates
505 extracted from Pyle (2011) for modelling applications. Our report presents the full range of data
506 in Pyle's work and notes that rates can be ~ 0.2 div d^{-1} higher than the values used by Follet et al.
507 (2018) depending on the strain used. These higher rates are consistent with the mechanistic
508 model of Inomura et al. (2020) in that host carbon fixation is substantial enough support to the
509 symbiont N_2 fixation rates required for the unit DDA growth. This host derived carbon is likely
510 to also be the reductant and energy source required to support the lengthy decline of N_2 fixation
511 rates at the beginning of the scotophase noted in the diel experiment (Fig. 4). Further
512 experimental verification is required.

513 When comparing rates, the possibility of strain-specific variation between Foster et al.'s
514 (2011) Pacific Ocean collections, Carpenter et al.'s (1999) field collections and our Gulf of
515 Mexico isolations cannot be excluded. Symbionts of the 3 diatom host genera have diverged
516 with strong host specificity within diatom host genera (Foster & Zehr 2006; Janson et al. 1999).
517 Bar Zeev et al. (2008) noted evidence of seasonally varying *Hemiaulus*-DDA dominated
518 *Richelia* clades in the Mediterranean but there is little data to assess how physiological
519 characteristics vary with habitat. *Rhizosolenia* and *Hemiaulus* DDA symbionts appear limited to
520 vertical transmission during division or possibly transmission during auxosporulation (Foster &
521 Zehr 2019) raising the possibility of genetic drift of various degrees within populations (Bar-
522 Zeev et al. 2008).
523
524 Conclusions
525 Two symbiotic associations between host diatoms and their intracellular heterocystous
526 cyanobacterium (*Hemiaulus hauckii* - *Richelia intracellularis* and *Hemiaulus membranaceus*-
527 *Richelia intracellularis*) were successfully cultured for up to 3 years on artificial seawater
528 medium. The N_2-fixation and growth rate data provided here are, to our knowledge, the first
529 published laboratory-based data for the *Hemiaulus* DDA. This work provides details on isolation
530 techniques that proved key to successful culturing. The symbioses are sensitive to handling,
531 requiring rapid collection and isolation for successful growth. The cultures did not undergo
532 sexual reproduction, and the lack of auxosporulation and concurrent size increase is a barrier to
533 long-term stable culture. Both symbioses grow without added nitrogen other than dissolved N_2
534 and are supported at maximum growth rates solely by symbiont nitrogen fixation. Maximum
535 growth rates of the intact diatom-cyanobacterium symbiosis are < 1 div d^{-1} and are similar to the

reported rates for another diatom-cyanobacterium symbiosis (*Rhizosolenia clevei-Richelia intracellularis*). Unlike the *Rhizosolenia clevei-Richelia intracellularis* symbiosis, the *H. hauckii – Richelia intracellularis* symbiosis does not assimilate nitrate. Nitrogen fixation by the heterocystous symbiont while within the host diatom has a clear diel pattern with maximum rates occurring during the photophase. The culture nitrogen fixation rates are consistent with field measured rates; however, maximum culture rates are ~6-8 times previously measured field rates. Both growth and nitrogen fixation rates follow light saturation kinetics. These data provide direct input for parameterization of light-dependent growth and nitrogen fixation in biogeochemical models.

Both literature reports and our isolation of a nitrate-utilizing, symbiont-free *Hemiaulus* culture are consistent with distinct symbiont-free and symbiont-containing lines of the diatom *Hemiaulus*. If correct, these different lineages would be useful models for understanding the evolution of these symbioses in diatoms.

References

Andersen RA, and Kawachi M. 2005. Chapter 6. Traditional Microalgal Isolation Techniques. In: Andersen RA, ed. *Algal Coulture Techniques*. Burlington, MA: Elsevier Acaemic Press, 83-100.

Bar-Zeev E, Yogev T, Man-Aharonovich D, Kress N, Herut B, Beja O, and Berman-Frank I. 2008. Seasonal dynamics of the endosymbiotic, nitrogen-fixing cyanobacterium *Richelia intracellularis* in the eastern Mediterranean Sea. *Isme Journal* 2:911-923. 10.1038/ismej.2008.56

Brand LE, and Guillard RRL. 1981. The effects of continuous light and light intensity on the reproduction rates of twenty-two species of marine phytoplankton. *Journal of Experimental Marine Biology and Ecology* 50:119-132.

Björkman, K. M., M. J. Church, J. K. Doggett, and D. M. Karl. 2015. Differential Assimilation of Inorganic Carbon and Leucine by *Prochlorococcus* in the Oligotrophic North Pacific Subtropical Gyre. Frontiers in Microbiology **6**(1401). 10.3389/fmicb.2015.01401

565 Brzezinski MA, Villareal TA, and Lipschultz F. 1998. Silica production and the contribution of
566 diatoms to new and primary production in the central North Pacific. *Marine Ecology*
567 *Progress Series* 167:89-104.
568 Campbell L, Olson RJ, Sosik HM, Abraham A, Henrichs DW, Hyatt CJ, and Buskey EJ. 2010.
569 First harmful *Dinophysis* (Dinophyceae, Dinophyceales) bloom in the U.S. is revealed by
570 automated imaging flow cytometry. *Journal of Phycology* 46:66-75. 10.1111/j.1529-
571 8817.2009.00791.x
572 Campbell, L., D.W. Henrichs, E.E. Peacock, J. Futrelle and H.M. Sosik. 2017. Imaging
573 FlowCytobot provides novel insights on phytoplankton community dynamics. Pages 74-
574 70. In: Proenca, L. A. O. and Hallegraeff, G. (eds). Marine and Fresh-Water Harmful
575 Algae. Proceedings of the 17th International Conference on Harmful Algae. International
576 Society for the Study of Harmful Algae and Intergovernmental Oceanographic
577 Commission of UNESCO 2017. ISBN 978-87-990827-6-6.
578 Caputo A, Nylander JAA, and Foster RA. 2019. The genetic diversity and evolution of diatom-
579 diazotroph associations highlights traits favoring symbiont integration. *FEMS*
580 *Microbiology Letters* 366:fny297. 10.1093/femsle/fny297
581 Carpenter EJ. 2002. Marine cyanobacterial symbioses. *Biology and Environment* 102B:15-18.
582 10.3318/bioe.2002.102.1.15
583 Carpenter EJ, and Janson S. 2000. Intracellular cyanobacterial symbionts in the marine diatom
584 *Climacodium frauenfeldianum* (Bacillariophyceae). *Journal of Phycology* 36:540-544.
585 Carpenter EJ, Montoya JP, Burns J, Mulholland MR, Subramaniam A, and Capone DG. 1999.
586 Extensive bloom of a N_2-fixing diatom/cyanobacterial association in the tropical Atlantic
587 Ocean. *Marine Ecology-Progress Series* 185:273-283.
588 Cooley SR, Coles VJ, Subramaniam A, and Yager PL. 2007. Seasonal variations in the Amazon
589 plume-related atmospheric carbon sink. *Global Biogeochemical Cycles* 21.
590 10.1029/2006gb002831
591 Dore JE, Letelier RM, Church MJ, Lukas R, and Karl DM. 2008. Summer phytoplankton blooms
592 in the oligotrophic North Pacific Subtropical Gyre: Historical perspective and recent
593 observations. *Progress in Oceanography* 76:2-38.
594 Eppley RW, and Peterson BJ. 1979. Particulate organic matter flux and planktonic new
595 production in the deep ocean. *Nature (London)* 282:677-680.
596 Farnelid H, Turk-Kubo K, Ploug H, Ossolinski JE, Collins JR, Van Mooy BAS, and Zehr JP.
597 2019. Diverse diazotrophs are present on sinking particles in the North Pacific
598 Subtropical Gyre. *The ISME Journal* 13:170-182. 10.1038/s41396-018-0259-x
599 Follett CL, Dutkiewicz S, Karl DM, Inomura K, and Follows MJ. 2018. Seasonal resource
600 conditions favor a summertime increase in North Pacific diatom–diazotroph associations.
601 *The ISME Journal*. 10.1038/s41396-017-0012-x
602 Fong AA, Karl DM, Lukas R, Letelier RM, Zehr JP, and Church MJ. 2008. Nitrogen fixation in
603 an anticyclonic eddy in the oligotrophic North Pacific Ocean. *Isme Journal* 2:663-676.
604 10.1038/ismej.2008.22
605 Foster RA, Carpenter EJ, and Bergman B. 2006. Unicellular cyanobionts in open ocean
606 dinoflagellates, radiolarians, and tintinnids: Ultrastructural characterization and immuno-
607 localization of phycoerythrin and nitrogenase. *Journal of Phycology* 42:453-463.
608 Foster RA, Goebel NL, and Zehr JP. 2010. Isolation of *Calothrix rhizosoleniae* (Cyanobacteria)
609 strain SC01 from *Chaetoceros* (Bacillariophyta) spp. diatoms of the subtropical North
610 Pacific Ocean. *Journal of Phycology* 46:1028-1037. 10.1111/j.1529-8817.2010.00885.x

611 Foster RA, Kuypers MMM, Vagner T, Paerl RW, Musat N, and Zehr JP. 2011. Nitrogen fixation
612 and transfer in open ocean diatom-cyanobacterial symbioses. *Isme Journal* 5:1484-1493.
613 10.1038/ismej.2011.26
614 Foster RA, and O'Mullan GD. 2008. Nitrogen-fixing and nitrifying symbioses in the marine
615 environment. In: Capone DG, Bronk DA, Mulholland MR, and Carpenter EJ, eds.
616 *Nitrogen in the Marine Environment, 2nd Edition*. San Diego: Elsevier, 1197-1218.
617 Foster RA, Subramaniam A, Mahaffey C, Carpenter EJ, Capone DG, and Zehr JP. 2007.
618 Influence of the Amazon River plume on distributions of free-living and symbiotic
619 cyanobacteria in the western tropical north Atlantic Ocean. *Limnology and*
620 *Oceanography* 52:517-532.
621 Foster RA, Subramaniam A, and Zehr JP. 2009. Distribution and activity of diazotrophs in the
622 Eastern Equatorial Atlantic. *Environmental Microbiology* 11:741-750. 10.1111/j.1462-
623 2920.2008.01796.x
624 Foster RA, and Zehr JP. 2006. Characterization of diatom-cyanobacteria symbioses on the basis
625 of nifH, hetR and 16S rRNA sequences. *Environmental Microbiology* 8:1913-1925.
626 10.1111/j.1462-2920.2006.01068.x
627 Foster RA, and Zehr JP. 2019. Diversity, Genomics, and Distribution of Phytoplankton-
628 Cyanobacterium Single-Cell Symbiotic Associations. *Annual Review of Microbiology*
629 73:435-456. 10.1146/annurev-micro-090817-062650
630 Furnas MJ. 1991. Net in situ growth rates of phytoplankton in an oligotrophic, tropical shelf
631 ecosystem. *Limnology and Oceanography* 36:13-29.
632 Grasshoff, K. K., K. Kremling, and M. Ehrhardt., editors. 1999. Methods of Seawater Analysis.
633 Wiley-VCH. Verlag GmbH, D-69469 Weinheim (Federal Republic of Germany), 599 pp.
634 Grosse J, Bombar D, Hai ND, Lam NN, and Voss M. 2009. The Mekong River plume fuels
635 nitrogen fixation and determines phytoplankton species distribution in the South China
636 Sea during low- and high-discharge season. *Limnology and Oceanography* 55:1668-
637 1680. 10.4319/lo.2010.55.4.1668
638 Guillard RRL. 1973. Division rates. In: Stein JR, ed. *Handbook of Phycological Methods Culture*
639 *Methods and Growth Measurements*. New York: Cambridge University Press, 290-320.
640 Hallegraeff GM, and Jeffrey SW. 1984. Tropical phytoplankton species and pigments of
641 continental shelf waters of North and North-west Australia. *Marine Ecology-Progress*
642 *Series* 20:59-74.
643 Harding K, Turk-Kubo KA, Sipler RE, Mills MM, Bronk DA, and Zehr JP. 2018. Symbiotic unicellular
644 cyanobacteria fix nitrogen in the Arctic Ocean. *Proceedings of the National Academy of Sciences*
645 *of the United States of America* 115:13371-13375. 10.1073/pnas.1813658115
646 Harke MJ, Frischkorn KR, Haley ST, Aylward FO, Zehr JP, and Dyhrman ST. 2019. Periodic
647 and coordinated gene expression between a diazotroph and its diatom host. *The ISME*
648 *Journal* 13:118-131. 10.1038/s41396-018-0262-2
649 Heinbokel, J. F. 1986. Occurrence of *Richelia intracellularis* (Cyanophyta) within the diatoms
650 *Hemiaulus hauckii* and *H. membranaceus* off Hawaii. Journal of Phycology **22**:399-403.
651 Hilton JA, Foster RA, Tripp HJ, Carter BJ, Zehr JP, and Villareal TA. 2013. Genomic deletions
652 disrupt nitrogen metabolism pathways of a cyanobacterial diatom symbiont. *Nature*
653 *Communications* 4:1767-1767. 10.1038/ncomms2748
654 Holl CM, and Montoya JP. 2005. Interactions between nitrate uptake and nitrogen fixation in
655 continuous cultures of the marine diazotroph *Trichodesmium* (Cyanobacteria). *Journal of*
656 *Phycology* 41:1178-1183.

Inomura K, Bragg J, Riemann L, and Follows MJ. 2018. A quantitative model of nitrogen fixation in the presence of ammonium. *PLoS ONE* 13:e0208282. 10.1371/journal.pone.0208282

Inomura K, Follett CL, Masuda T, Eichner M, Prasil O, and Deutsch C. 2020. Carbon transfer from the host diatom enables fast growth and high rate of N_2 Fixation by symbiotic heterocystous cyanobacteria. *Plants-Basel* 9:16. 10.3390/plants9020192

Janson S, Wouters J, Bergman B, and Carpenter EJ. 1999. Host specificity in the *Richelia* - diatom symbiosis revealed by hetR gene sequence analysis. *Environmental Microbiology* 1:431-438.

Karl DM, Church MJ, Dore JE, Letelier RM, and Mahaffey C. 2012. Predictable and efficient carbon sequestration in the North Pacific Ocean supported by symbiotic nitrogen fixation. *Proceedings of the National Academy of Sciences* 109:1842-1849.

Karsten G. 1905. Das phytoplankton des Atlantischen Ozeans nach dem material der deutschen Tiefsee-Expedition 1898-1899. *Wissen Erg Deut Tiefsee-Exped "VALDIVA" 1898-1899* 2:137-219.

Klawonn I, Eichner MJ, Wilson ST, Moradi N, Thamdrup B, Kümmel S, Gehre M, Khalili A, Grossart H-P, Karl DM, and Ploug H. 2020. Distinct nitrogen cycling and steep chemical gradients in *Trichodesmium* colonies. *The ISME Journal* 14:399-412. 10.1038/s41396-019-0514-9

Kranzler CF, Krause JW, Brzezinski MA, Edwards BR, Biggs WP, Maniscalco M, McCrow JP, Van Mooy BAS, Bidle KD, Allen AE, and Thamatrakoln K. 2019. Silicon limitation facilitates virus infection and mortality of marine diatoms. *Nature Microbiology*. 10.1038/s41564-019-0502-x

Mills MM, Turk-Kubo KA, van Dijken GL, Henke BA, Harding K, Wilson ST, Arrigo KR, and Zehr JP. 2020. Unusual marine cyanobacteria/haptophyte symbiosis relies on N_2fixation even in N-rich environments. *Isme Journal*:12. 10.1038/s41396-020-0691-6

Mulholland MR, and Capone DG. 2000. The nitrogen physiology of the marine N_2-fixing cyanobacteria *Trichodesmium* spp. *Trends in Plant Science* 5:148-153.

Pyle A. 2011. Light Dependant Growth and Nitrogen Fixation Rates in the *Hemiaulus hauckii* and *Hemiaulus membranaceus* Diatom-Diazotroph Associations M.S. thesis. The University of Texas at Austin. 77 pp.

Scharek R, Latasa M, Karl DM, and Bidigare RR. 1999. Temporal variations in diatom abundance and downward vertical flux in the oligotrophic North Pacific gyre. *Deep-Sea Research Part I-Oceanographic Research Papers* 46:1051-1075.

Schouten S, Villareal T, Hopmans E, Mets A, Swanson K, and Damste J. 2013. Endosymbiotic heterocystous cyanobacteria synthesize different heterocyst glycolipids than free-living heterocystous cyanobacteria. *Phytochemistry* 85:115-121.

Schöne HK, and Schöne A. 1982. MET 44: A weakly enriched sea-water medium for ecological sudies on marine plankton algae, and some examples of its application. *Botanica Marina* 25:117-122.

Stukel MR, Coles VJ, Brooks MT, and Hood RR. 2014. Top-down, bottom-up and physical controls on diatom-diazotroph assemblage growth in the Amazon River plume. *Biogeosciences* 11:3259-3278. 10.5194/bg-11-3259-2014

Subramaniam A, Yager PL, Carpenter EJ, Mahaffey C, Bjorkman K, Cooley S, Kustka AB, Montoya JP, Sanudo-Wilhelmy SA, Shipe R, and Capone DG. 2008. Amazon River enhances diazotrophy and carbon sequestration in the tropical North Atlantic Ocean.

Proceedings of the National Academy of Sciences of the United States of America 105:10460-10465. 10.1073/pnas.0710279105

Taylor FJR. 1982. Symbioses in marine microplankton. *Ann Inst Océanogr, Paris* 58 S:61-90.

Tomkins, M., A. P. Martin, A. J. G. Nurser, and T. R. Anderson. 2020. Phytoplankton acclimation to changing light intensity in a turbulent mixed layer: A Lagrangian modelling study. Ecological Modelling **417**:108917.

van Tol HM, Amin SA, and Armbrust EV. 2017. Ubiquitous marine bacterium inhibits diatom cell division. *Isme Journal* 11:31-42. 10.1038/ismej.2016.112

Venrick EL. 1974. The distribution and significance of *Richelia intracellularis* Schmidt in the North Pacific Central Gyre. *Limnology and Oceanography* 19:437-445.

Villareal TA. 1989. Division cycles in the nitrogen-fixing *Rhizosolenia* (Bacillariophyceae)-*Richelia* (Nostocaceae) symbiosis. *British Phycological Journal* 24:357-365.

Villareal TA. 1990. Laboratory cultivation and preliminary characterization of the *Rhizosolenia* (Bacillariophyceae)-*Richelia* (Cyanophyceae) symbiosis. *Marine Ecology-Pubblicazioni Della Stazione Zoologica Di Napoli I* 11:117-132.

Villareal TA. 1991. Nitrogen fixation by the cyanobacterial symbiont of the diatom genus *Hemiaulus*. *Marine Ecology Progress Series* 76:201-204.

Villareal TA. 1992. Marine nitrogen-fixing diatom-cyanobacterial symbioses. In: Carpenter EJ, Capone DG, and Reuter J, eds. *Marine Pelagic Cyanobacteria: Trichodesmium and other Diazotrophs*. Netherlands: Kluwer, 163-175.

Villareal TA. 1994. Widespread occurrence of the *Hemiaulus*-cyanobacterial symbiosis in the Southwest North Atlantic Ocean. *Bull Mar Sci* 53:1-7.

Villareal TA, Adornato L, Wilson C, and Shoenbachler CA. 2011. Summer blooms of diatom-diazotroph assemblages (DDAs) and surface chlorophyll in the N. Pacific gyre – a disconnect. *Journal of Geophysical Research-Oceans* 116:DOI: 10.1029/2010JC006268. 10.1029/2010JC006268

Villareal TA, Brown CG, Brzezinski MA, Krause JW, and Wilson C. 2012. Summer diatom blooms in the North Pacific subtropical gyre: 2008-2009. *PLoS ONE* 7:e33109. doi:33110.31371/journal.pone.0033109.

Weber SC, Carpenter EJ, Coles VJ, Yager PL, Goes J, and Montoya JP. 2017. Amazon River influence on nitrogen fixation and export production in the western tropical North Atlantic. *Limnology and Oceanography* 62:618-631. 10.1002/lno.10448

Welschmeyer NA. 1994. Fluorometric analysis of chlorophyll a in the presence of chlorophyll b and pheopigments. *Limnology and Oceanography* 39:1985-1992.

White AE, Spitz YH, and Letelier RM. 2007. What factors are driving summer phytoplankton blooms in the North Pacific Subtropical Gyre? *Journal of Geophysical Research-Oceans* 112:doi:10.1029/2007JC004129.

Wilson C, Villareal TA, and Bogard SJ. 2004. Large-scale forcing of late summer chlorophyll blooms in the oligotrophic Pacific. *AGU Winter meeting, 13-17 Dec 2005, San Francisco, CA*.

Wilson C, Villareal TA, Maximenko N, Montoya JP, Bograd SJ, and Schoenbaechler CA. 2008. Biological and physical forcings of late summer chlorophyll blooms at 30º N in the oligotrophic Pacific. *Journal of Marine Systems* 69:164–176.

Yeung LY, Berelson WM, Young ED, Prokopenko MG, Rollins N, Coles VJ, Montoya JP, Carpenter EJ, Steinberg DK, Foster RA, Capone DG, and Yager PL. 2012. Impact of

diatom-diazotroph associations on carbon export in the Amazon River plume. *Geophysical Research Letters* 39:L18609. 10.1029/2012gl053356

Zehr, J. P., J. P. Montoya, B. D. Jenkins, I. Hewson, E. Mondragon, C. M. Short, M. J. Church, A. Hansen, and D. M. Karl. 2007. Experiments linking nitrogenase gene expression to nitrogen fixation in the North Pacific subtropical gyre. Limnology and Oceanography **52**:169-183.

Zehr JP, and Capone DG. 2020. Changing perspectives in marine nitrogen fixation. *Science (Washington, DC)* 368:729-+. 10.1126/science.aay9514

Zehr JP. 2011. Nitrogen fixation by marine cyanobacteria. *Trends in Microbiology* 19:162-173. 10.1016/j.tim.2010.12.004

Zhu, Z., F. X. Fu, P. P. Qu, E. W. K. Mak, H. B. Jiang, R. F. Zhang, Z. Y. Zhu, K. S. Gao, and D. A. Hutchins. 2020. Interactions between ultraviolet radiation exposure and phosphorus limitation in the marine nitrogen-fixing cyanobacteria *Trichodesmium* and *Crocosphaera*. Limnology and Oceanography **65**:363-376.

Table 1(on next page)

Results from the modified hyperbolic tangent function growth rate-irradiance and hyperbolic tangent function N_2-fixation-irradiance curve fit.

The three N_2-fixation experiments were adapted to the given light levels for 7 days. The growth rate experiments were adapted at each of the light levels for 7 days. Strain 91 was used in these experiments

1

Measurement	Incubation E [1]	Initial slope (α)	Realized maximum rate	E_c[1]	E_k [1]	R^2
N_2 fixation	50	2.079[2]	84	-	41	0.75
N_2 fixation	150	0.905[2]	155[4]	-	170	0.95
N_2 fixation	200	1.197[2]	144[4]	-	120	0.97
Growth Rate	Light gradient	0.009[3]	0.76[5]	15	84	0.99
Growth Rate	Light gradient	0.009[3]	0.93[5]	7	110	0.99

2

3 [1] $\mu mol\ m^{-2}\ s^{-1}$

4 [2] $(fmol\ N\ heterocyst^{-1}\ h^{-1})(\mu mol\ m^{-2}\ s^{-1})^{-1}$

5 [3] $(div\ d^{-1})(\mu mol\ m^{-2}\ s^{-1})^{-1}$

6 [4] $(fmol\ N\ heterocyst^{-1}\ h^{-1})$

7 [5] $div\ d^{-1}$

Figure 1

Photomicrographs of *Hemiaulus membranaceus* (A,B) and *H. hauckii* (C, D) symbioses cultured in this study.

Images are paired photomicrographs of transmitted light micrographs (A, C) and light micrographs under epifluorescence (see methods) (B, D), and were taken from samples in a Sedgewick Rafter counting cell to minimize breakage of long chains. The vertical black bar in Fig. 1c is a marking from the Sedgewick Rafter cell. It lies under the chain; hence. it does not obscure details illuminated by epifluorescence in Fig. 1d. Scale bar = 200 µm for all images. Image credit: A.E Pyle

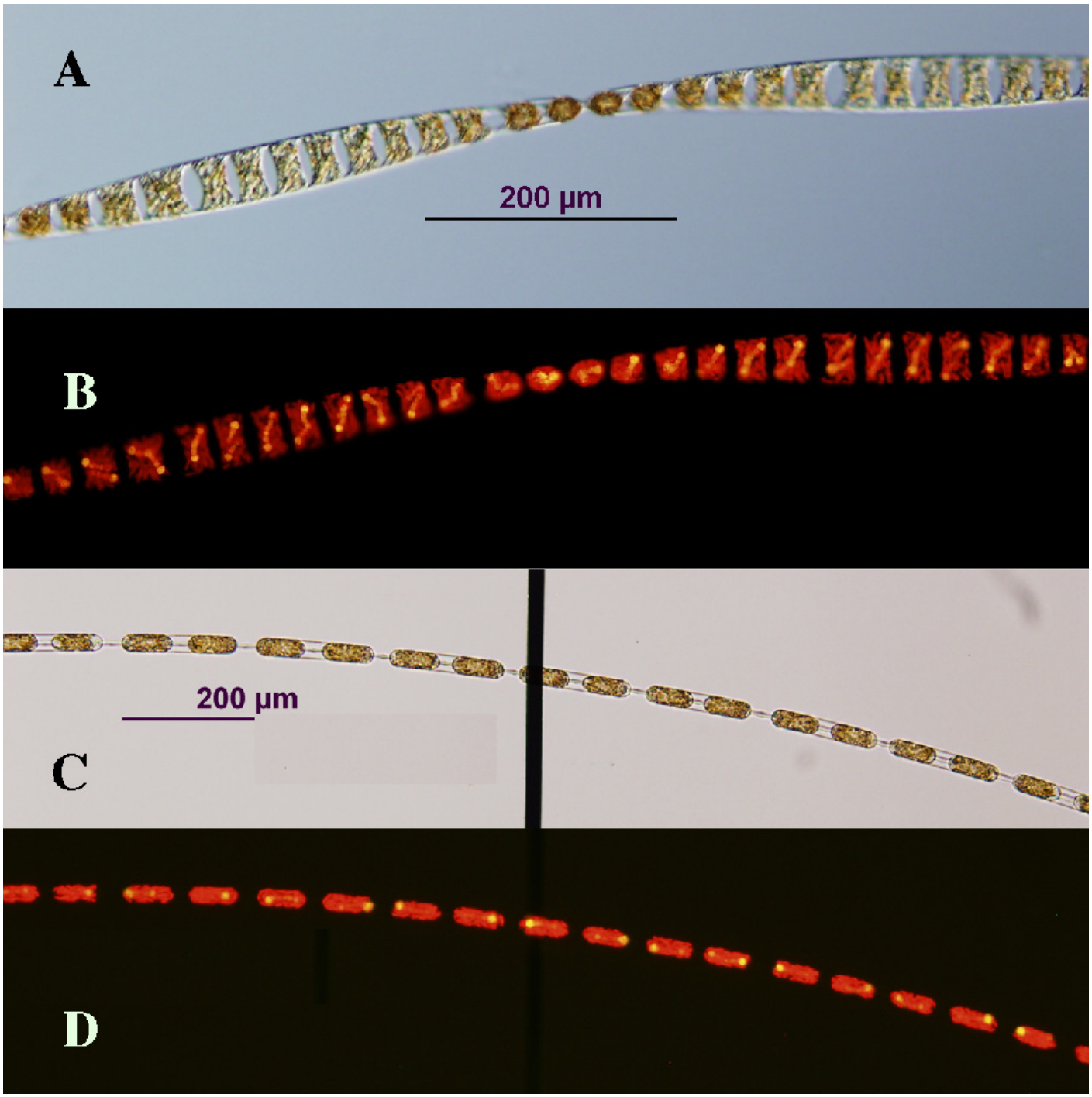
A
200 µm
B
200 µm
C
D

Figure 2

Typical *Hemiaulus hauckii* growth curve at two irradiance levels in modified YBC-II medium with no added nitrogen using strain #91.

A. Cell abundance and bulk chlorophyll *a* concentration. B. Chlorophyll *a* content per host cell (sum of host and symbiont chl *a*) and symbiont presence in hosts. High light (HL: 200 µmol m^{-2} s^{-1}); Low light (LL: 50 µmol m^{-2} s^{-1}). Values are means of duplicates ± standard deviation.

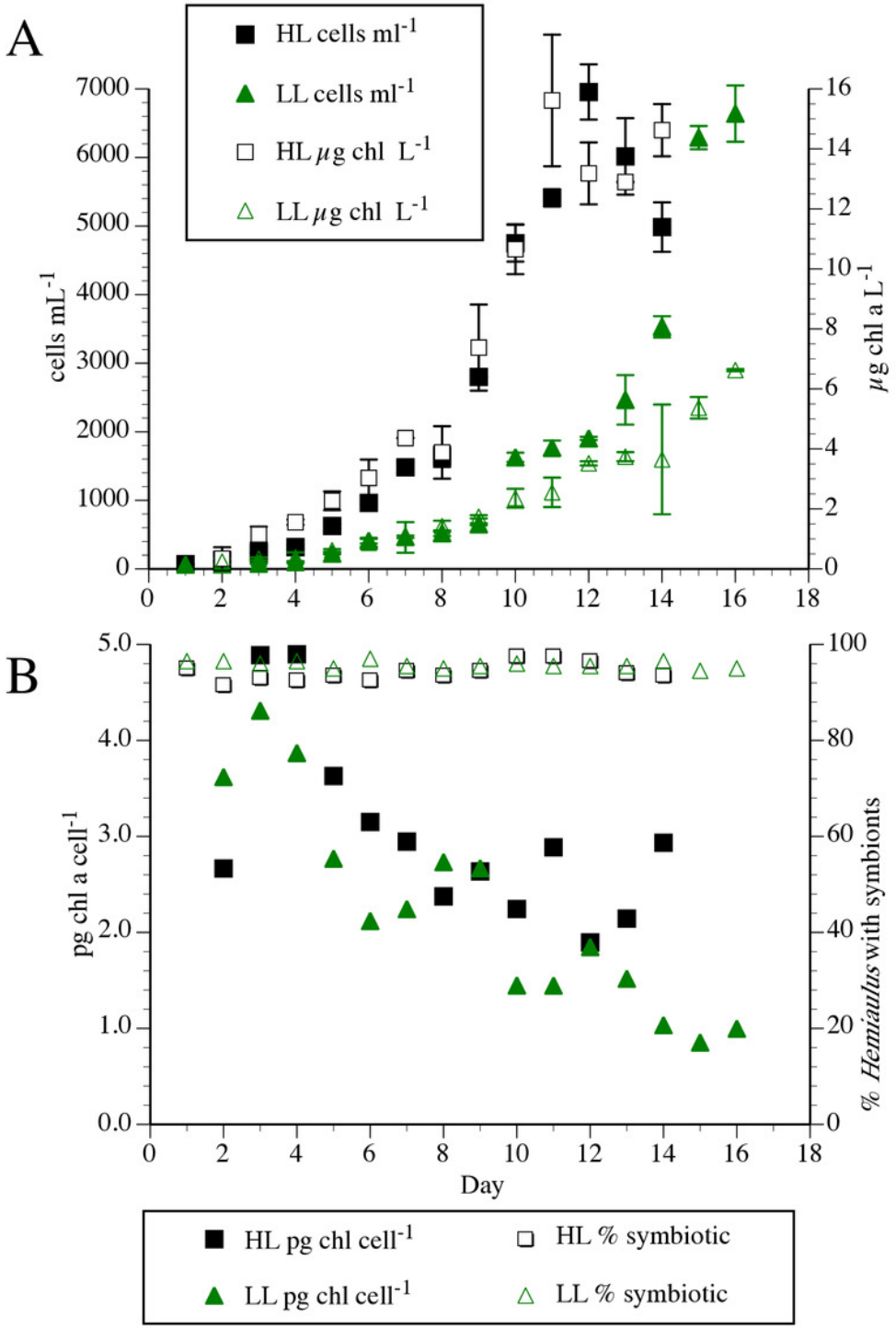
A
HL cells ml-1
LL cells ml-1
HL µg chl L-1
LL µg chl L-1
cells mL-1
µg chl a L-1
B
pg chl a cell-1
% Hemiaulus with symbionts
Day
HL pg chl cell-1
LL pg chl cell-1
HL % symbiotic
LL % symbiotic

Figure 3

Irradiance-growth rate relationships for *Hemiaulus hauckii* symbiosis strains #91 and #9.

Open circles and open squares are from strain #91 (7 points) in two separate experiments, solid squares (2 points) are from strain #9 measured approximately 1 year prior to strain #91. Error bars are 95% confidence intervals. Data from strain #91 are fit to a hyperbolic tangent function. Curve fit parameters are listed in Table 1 and in the Article S1.

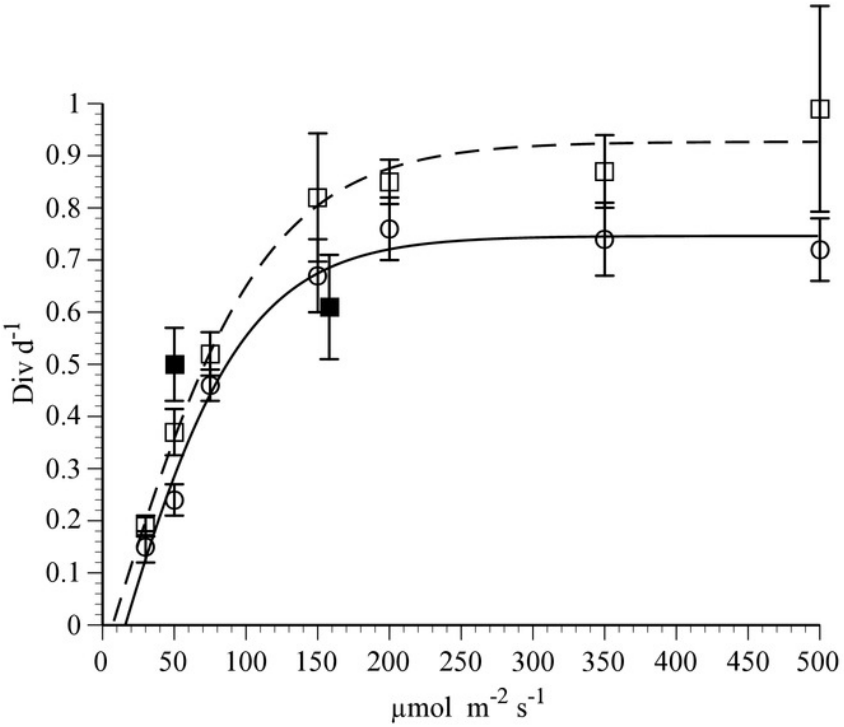
Div d-1
0
0.1
0.2
0.3
0.4
0.5
0.6
0.7
0.8
0.9
1
0
50
100
150
200
250
300
350
400
450
500
µmol m-2 s-1

Figure 4

Diel patterns of N_2 fixation in N-free medium.

(A) *Hemiaulus hauckii* symbiosis (Strain #92= black symbols; Strain #22= red symbol). (B) *H. membranaceus* symbiosis (Strain #82). Growth rates (*H. hauckii symbiosis*) were 0.35±0.05 div d^{-1} (strain #91) and 0.43 ±0.10 div d^{-1} (strain #22). Growth rate of the *H. membranaceus* symbiosis was 0.56±0.10 div d^{-1}. Dark bars indicate nighttime. Both cultures were grown at 200 µmol m^{-2} s^{-1}. See text for details of the methodology for the 4 h and 5 pt average measurements. Error bars are standard deviation.

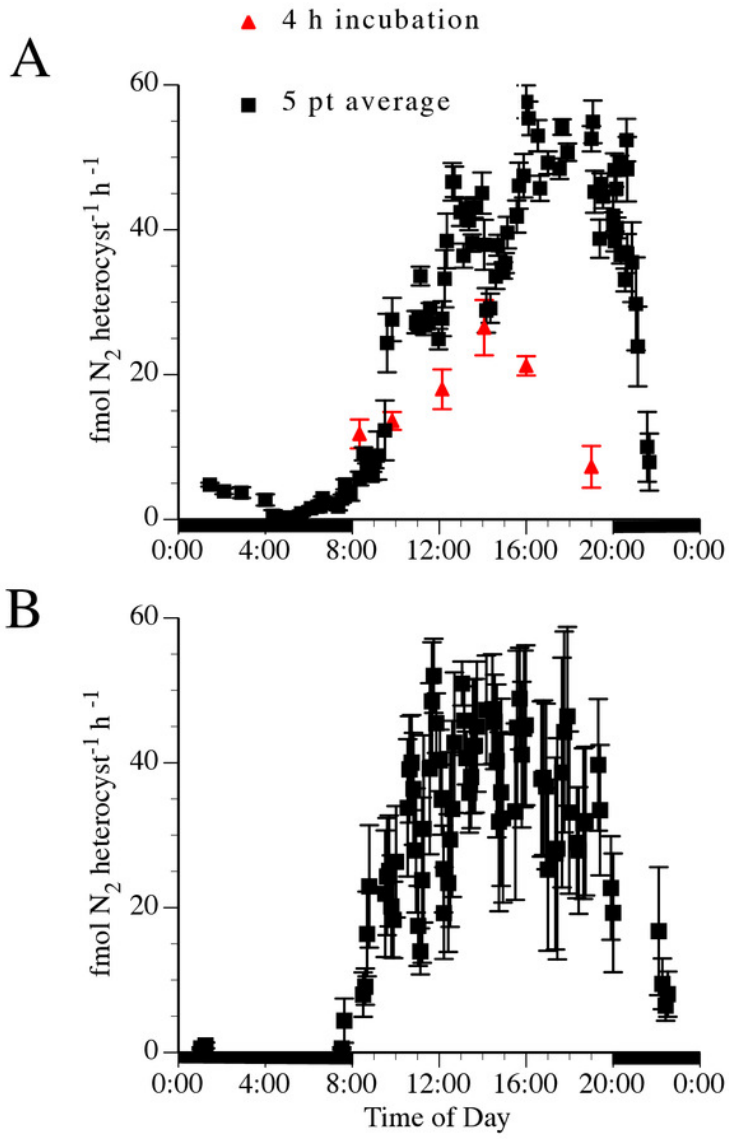
A
4 h incubation
5 pt average
fmol N_2 heterocyst^{-1} h^{-1}
60
40
20
0
0:00
4:00
8:00
12:00
16:00
20:00
0:00
B
fmol N_2 heterocyst^{-1} h^{-1}
60
40
20
0
0:00
4:00
8:00
12:00
16:00
20:00
0:00
Time of Day

Figure 5

Irradiance-N_2 fixation rate relationships for the *Hemiaulus hauckii* symbiosis (Strain #91) adapted to three light intensities.

Error bars are 95% confidence intervals.

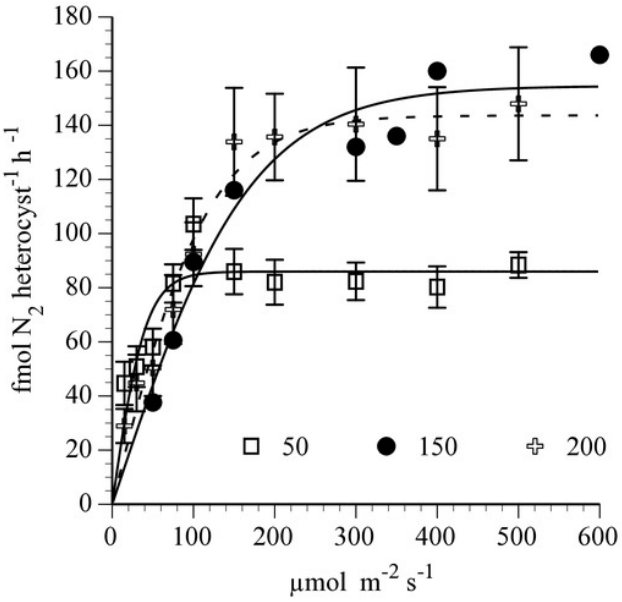
fmol N_2 heterocyst^{-1} h^{-1}
µmol m^{-2} s^{-1}
50
150
200
0
20
40
60
80
100
120
140
160
180
0
100
200
300
400
500
600

Figure 6

Hemiaulus hauckii symbiosis growth in modified YBC-II medium under 3 nitrogen sources (N_2, nitrate, ammonium; Strain #83)

(A) Nitrate concentrations with and without added nitrate. (B) Ammonium concentrations with and without added ammonium. (C) Phosphate concentrations in the three nutrient conditions. (D) Silicate concentrations in the three nutrient conditions. (E) Cell abundance in the three nutrient conditions. (F) %*Hemiaulus* with symbionts in the three nutrient conditions. Only two symbols are visible in panels A and B due to overlapping near-zero values.

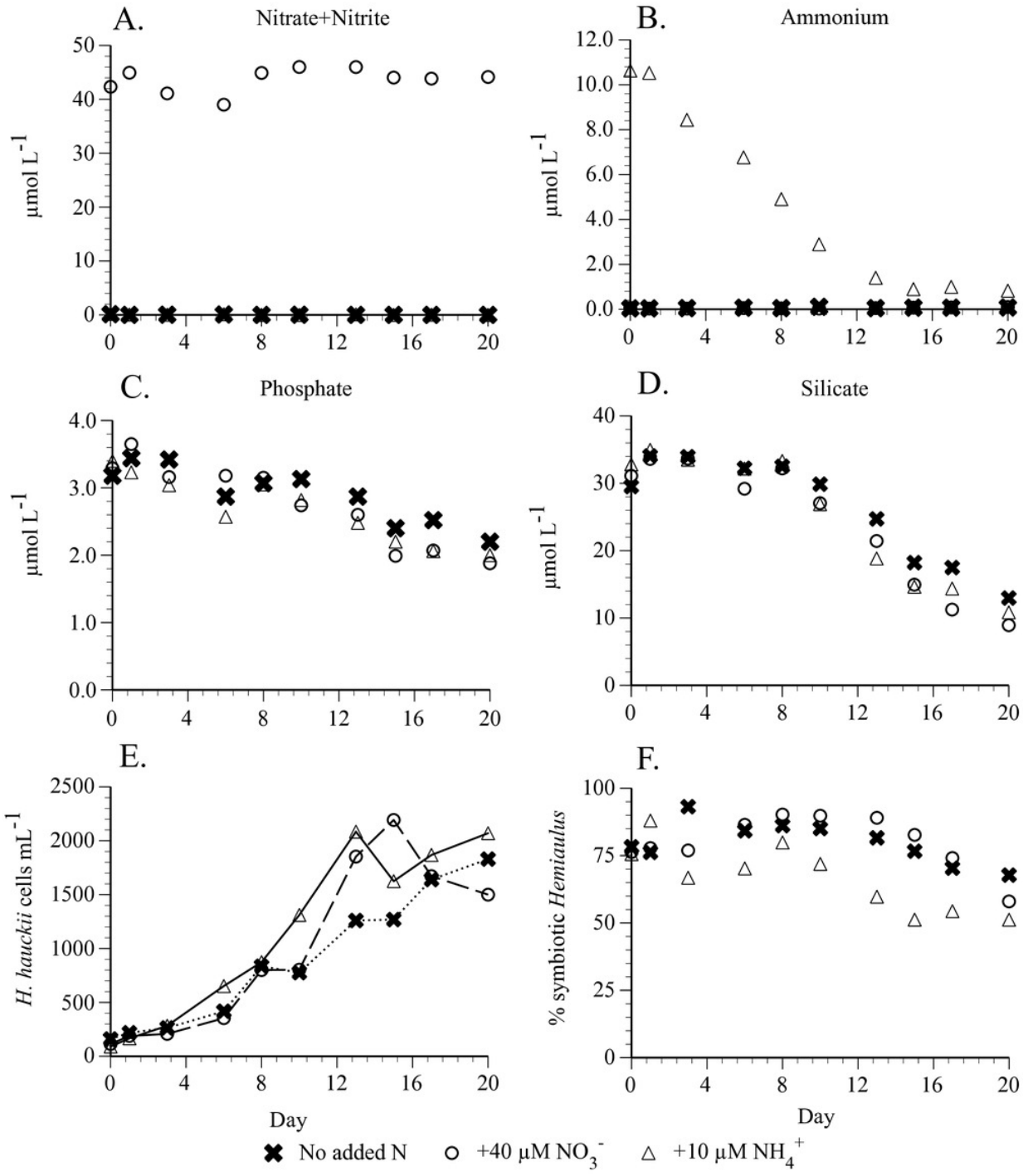
A.
Nitrate+Nitrite
µmol L-1
B.
Ammonium
µmol L-1
C.
Phosphate
µmol L-1
D.
Silicate
µmol L-1
E.
H. hauckii cells mL-1
F.
% symbiotic Hemiaulus
Day
Day
No added N
+40 µM NO3-
+10 µM NH4+